Geol. Mag. **146** (*2*), *2009, pp. 173–186. © 2008 Cambridge University Press*
doi:10.1017/S0016756808005499 *Printed in the United Kingdom*

Dehydration, melting and related garnet growth in the deep root of the Amalaoulaou Neoproterozoic magmatic arc (Gourma, NE Mali)

JULIEN BERGER*†‡§, RENAUD CABY¶, JEAN-PAUL LIÉGEOIS*, JEAN-CLAUDE C. MERCIER‡# & DANIEL DEMAIFFE†

*Musée royal de l'Afrique centrale, Section de géologie isotopique, Leuvensteenweg 13, B-3080 Tervuren, Belgique
†Université libre de Bruxelles (U.L.B.), Géochimie isotopique et géodynamique chimique, CP 160/02, av. F. Roosevelt 50, B-1050 Bruxelles, Belgique
‡Université de la Rochelle, UMR CNRS 6250 'LIENSs', ILE, 2 rue Olympe de Gouges F-17042 La Rochelle-cedex 1, France
¶Université de Montpellier 2, Laboratoire de Tectonophysique, Place E. Bataillon, F-34095 Montpellier-cedex, France
#Université de Nantes, UMR CNRS 6112 'LPGN', BP 92205, 2 rue de la Houssinière, F-44322 Nantes, France

(*Received* 13 February 2008; *accepted* 16 June 2008; First published online 17 September 2008)

Abstract – The Amalaoulaou Neoproterozoic island-arc massif belongs to the Gourma belt in Mali. The metagabbros and pyroxenites forming the main body of this arc root show the pervasive development of garnet. In the pyroxenites, the latter has grown by reaction between pyroxene and spinel during isobaric cooling. By contrast, in the metagabbros, garnet textures and relations to felsic veins exclude an origin through solid-state reactions only. It is proposed that garnet has grown following dehydration and localized melting of amphibole-bearing gabbros at the base of the arc. The plagioclase-saturated melts represented by anorthositic veins in the metagabbros and by trondhjemites in the upper part of the massif provide evidence for melting in the deep arc crust, which locally generated high-density garnet–clinopyroxene–rutile residues. Garnet growth and melting began around 850 °C at 10 kbar and the tonalitic melts were most probably generated around 1050 °C at $P \geq 10$ kbar. This HT granulitic imprint can be related to arc maturation, leading to a *P–T* increase in the deep arc root and dehydration and/or dehydration-melting of amphibole-bearing gabbros. Observation of such features in the root of this Neoproterozoic island arc has important consequences, as it provides a link to models concerning the early generation of continental crust.

Keywords: Gourma, dehydration-melting, island arc, Neoproterozoic, granulite.

1. Introduction

During Early Precambrian times, the major factories producing continental crust are thought to have been the magmatic arcs formed above subducting oceanic slabs (Taylor & McLennan, 1985; Rudnick, 1995). However, some debate exists about the effective contribution of island arcs in the generation of continental crust. Exposed island-arc sections are mainly basaltic (DeBari & Coleman, 1989; Dostal *et al.* 1996; Duclaux *et al.* 2006), and most of magma influx into arcs is basaltic in composition. This does not seem to be consistent with the andesitic composition of the continental crust; this is known as the arc paradox. One of the mechanisms proposed to explain this discrepancy is the melting of deep mafic rocks to form felsic melts and garnet–clinopyroxene residues (Garrido *et al.* 2006 and references therein). The formation of dense ultramafic residues or cumulates at the base of the arcs can lead to gravitational instability (Kay & Kay, 1988; Jull & Kelemen, 2001; Behn &Kelemen, 2006), that is, foundering of the dense lower arc crust into mantle (also referred to as lower crustal delamination), which may drive the bulk arc composition from basaltic to andesitic (Kelemen, Hanghoj & Greene, 2003; Kodaira *et al.* 2007).

The volcanic sections of recent oceanic and continental arcs have been extensively studied, and magmatic relics of middle and upper arc crust are sometimes preserved in Phanerozoic and Precambrian orogenic belts. By contrast, deep roots of magmatic arcs are much less commonly exposed and thus poorly understood, even if seismological constraints together with the occurrence of xenoliths in present-day arcs lava can provide valuable information about the whole arc structure (Kodaira *et al.* 2007). Despite the numerous studies on some scarce exposed Mesozoic arc roots, namely the Kohistan complex in Himalaya (Bard *et al.* 1980; Burg *et al.* 1998; Garrido *et al.* 2006), the Tonsina complex in Alaska (DeBari & Coleman, 1989; Greene *et al.* 2006) and the Fiordland massif in New Zealand (Mattinson, Kimbrough & Bradshaw, 1986; Hollis *et al.* 2003), little is known about Precambrian arc roots. Garnet granulites are always observed in these arc roots but their genesis is complex and several processes have been proposed to explain their formation: magmatic

§Author for correspondence: julien.berger@africamuseum.be

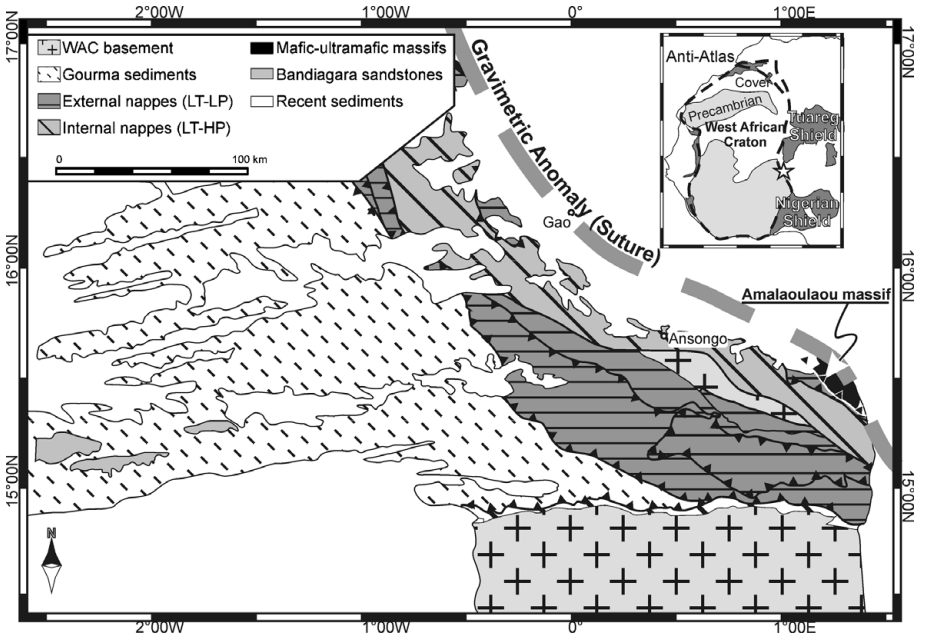

Figure 1. Location and geological map of the Gourma belt in NE Mali (map redrawn from Caby *et al.* 2008).

crystallization (Muntener & Ulmer, 2006), dehydration of deep hydrated mafic rocks (Bradshaw, 1989), melting of deep mafic rocks yielding a garnet-bearing residue (e.g. Garrido *et al.* 2006) and isobaric cooling of deep-seated gabbros (Ringuette, Martignole & Windley, 1999).

The Neoproterozoic Amalaoulaou island arc (NE Mali) shows assemblages from the deepest part of an island arc, and in this respect, it is an important key geological object. In particular, the Amalaoulaou arc root allows important observations about the genesis of garnet–clinopyroxene granulites and related felsic melts in arcs.

2. Geological setting and structure of the Amalaoulaou massif

2.a. The Gourma fold and thrust belt

The Amalaoulaou massif lies within the Gourma fold and thrust belt (Caby, 1979), a Pan-African collision zone between the West African Craton (WAC) and terranes exposed in the Tuareg shield (Black *et al.* 1994). The Gourma belt is structured in nappes thrust upon the folded terrigenous and carbonated Neoproterozoic sediments of the West African Craton passive margin (Fig. 1). The thrust-sheet stack comprises external nappes of metasedimentary material that underwent low-grade greenschist-facies metamorphism and internal nappes mainly made of metasedimentary rocks that evolved under LT–HP conditions (Caby, 1979; Caby *et al.* 2008); the Amalaoulaou massif is thrust over these two main tectonic units in easternmost Gourma. Relics of UHP coesite–eclogites (Caby, 1994; Jahn, Caby & Monié, 2001) have been found together with blueschists and eclogites in the Ansongo region (Caby *et al.* 2008). The UHP metamorphism has been dated at *c.* 623 Ma (Jahn, Caby & Monié, 2001); continental collision followed around 600 Ma. As for the Tilemsi island arc, which is located along the same suture in northern Mali (Caby, Andreopoulos-Renaud & Pin, 1989; Dostal, Dupuy & Caby, 1994), the Amalaoulaou massif coincides with a strong positive gravimetric anomaly (Bayer & Lesquer, 1978) which delineates the Pan-African suture on the eastern edge of the West African craton.

2.b. Structure of the Amalaoulaou massif

The Amalaoulaou massif is bounded to the south by a thrust contact against quartzites belonging to the external nappes. The northernmost outcrops of the massif progressively disappear underneath sediments from the Cretaceous Iullemeden basin and recent aeolian sands. The massif is composed of four ultrabasic–basic units (Fig. 2). These units have strongly dissimilar structural, lithological and metamorphic features (see below) and the contacts between the differents parts have never been observed in the field. This suggests that the Amalaoulaou massif is made of a stack of tectonic slices rather than being a single continuous lithological section.

The three different tectonic units identified are successively described from bottom to top:

(1) A lower sole of strongly deformed and totally serpentinized harzburgites and dunites. This unit is cut across by rodingitized mafic dykes, and the ultramafic rocks are partly transformed into Fe-jasper.
(2) An upper sole of strongly foliated and retrogressed epidote–garnet amphibolite with accessory

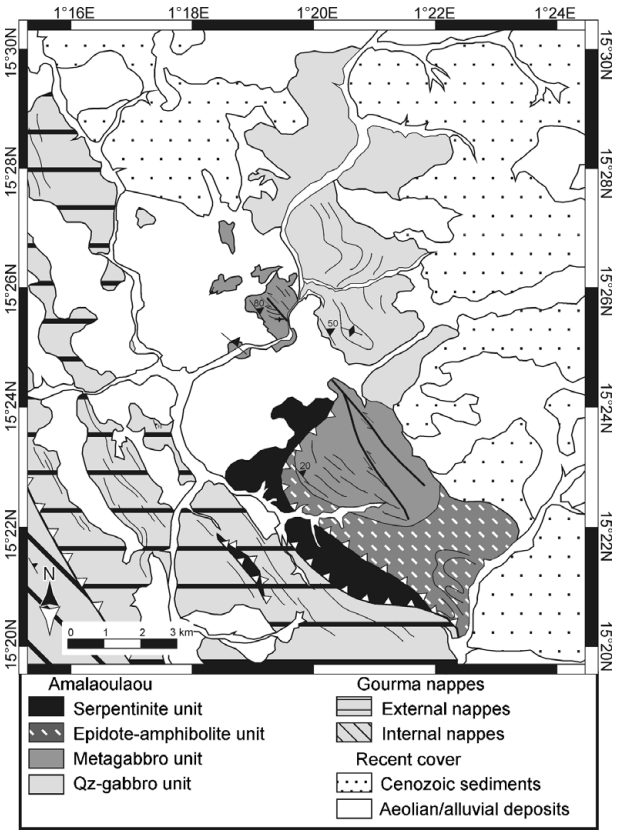

Figure 2. Geological map of the basic–ultrabasic Amalaoulaou massif in Gourma. The different units are in thrust contact.

paragonite, phengite, rutile, chloritoid, apatite and quartz. Discrete mylonitic actinolite–chlorite schists have been observed in this unit. Garnet porphyroclasts have core compositions similar to that observed in the overlying metagabbros, but the rim compositions result from low-temperature medium-pressure re-equilibration during exhumation of the massif. The rocks from this unit are most probably former metagabbros that underwent LT–MP conditions corresponding to those of the epidote–amphibolite facies.

(3) The main mass of layered metagabbros with variable modal proportions of magmatic clinopyroxene + orthopyroxene + plagioclase + rutile + apatite ± quartz assemblages that underwent several stages of deformation and metamorphism. Local preservation of high-Ti pargasite as inclusions in clinopyroxene seems to indicate that magmatic amphibole was present as an accessory or minor phase. Localized garnet growth under static granulitic conditions led to the development of a significant volume of garnet metagabbros. Deformation post-dating garnet growth was accompanied by solid-state recrystallization illustrating an evolution towards transitional granulite–amphibolite facies conditions. Syn-kinematic brown hornblende was formed at this stage; it clearly replaces both the magmatic and the recrystallized clinopyroxene. The metamorphic foliation of the metagabbros is defined by the shape preferred orientation of this amphibole (Fig. 4b). This deformation and recrystallization event deeply overprints the whole metagabbro unit and most of the rocks only show relict pyroxenes preserved from amphibolitization. Numerous centimetre-thick proto- to ultramylonitic bands were formed under the same conditions and are oblique to the main foliation. Some discrete mylonitic shear zones show amphibolite (Hbl–Pl–Ttn: mineral abbreviations following Spear, 1993) to greenschist (Chl–Act–Qtz–Ab) assemblages. Fresh plagioclase has never been observed anywhere in the whole massif; it has been totally replaced by fine intergrowths of epidote (80–90 vol. %), albite (10–20 vol. %) and white mica (including paragonite). Two generations of pyroxenites have been observed in the metagabbro mass. The earliest ones are lenses concordant with the metamorphic foliation, and some late pyroxenites cut across the HT foliation. Clinopyroxene is dominant with up to 15 % spinel and orthopyroxene. Garnet occurs as coronas around spinel and results from reaction between clinopyroxene and pleonaste. This structural unit is also characterized by the presence of numerous millimetre- to centimetre-thick anorthosite veins that are sometimes associated with garnet–clinopyroxene–rutile assemblages, these two associations being described in detail below.

(4) Leucogabbros and quartz–gabbros (Pl–Cpx–Qtz–Hbl–Ap–Zrn) together with minor tonalite, trondhjemite, hornblende–dolerite and hornblende–gabbro with partially preserved magmatic textures are found in the eastern part of the exposed massif. Quartz–gabbros are pyroxene–plagioclase–quartz rocks with minor proportions of ilmenite and apatite. The modal proportion of quartz is always higher than 10 vol. %. These rocks are free of pervasive deformation and metamorphism, though small brown hornblende blebs do replace clinopyroxene at crystal borders. Plagioclase is also totally transformed into secondary hydrous minerals. Hornblende gabbros have magmatic textures with a (retrogressed) plagioclase–hornblende–ilmenite magmatic assemblage. Two types of tonalite have been found. The first is a gneissic tonalite with quartz (∼ 25 vol. %), amphibole, retrogressed plagioclase, minor apatite and Ti-magnetite; the second type is a leucotonalite (trondhjemite) composed only of quartz (∼ 55 vol. %) and retrogressed plagioclase with partially preserved euhedral shapes. Fresh plagioclase was never observed either in this unit, or in the Amalaoulaou massif as a whole.

The structural position, the lithological section and the petrographical features of the Amalaoulaou massif are comparable to what has been found in exposed island-arc roots (Kohistan, Tonsina, Fiordland). Our new unpublished geochemical data also show that most of the Amalaoulaou metagabbros have the same

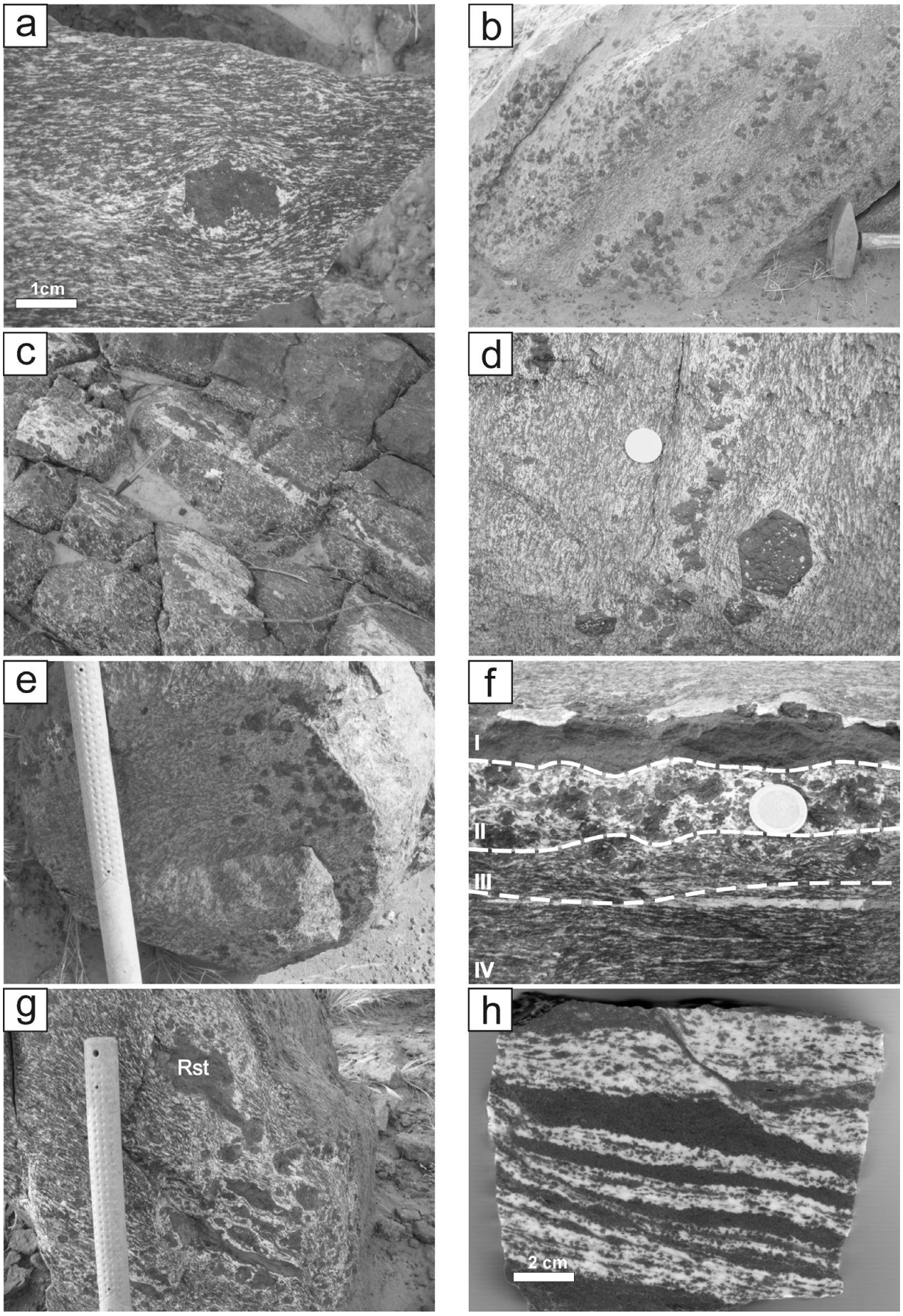

Figure 3. Illustration of the different modes of garnet occurrence in the Amalaoulaou metagabbros: (a) typical garnet in the metagabbros; it is surrounded by a plagioclase halo and has rare plagioclase inclusions; (b) disseminated garnet in the metagabbros (the hammer head is about 0.12 m long); (c) coarse garnets developed within or at the border of a deformed anorthositic vein (the pencil is 0.15 m long); (d) trail of poikiloblastic garnets enclosed in a felsic vein (the coin is 20 mm across); a coarse euhedral garnet surrounded by a

trace element pattern as some island-arc rocks (see Section 7). The Amalaoulaou massif can thus be interpreted as a piece of a deep arc root thrust onto the West African craton during the Pan-African orogeny. The magmatic crystallization of the metagabbroic suite is poorly dated at 801 ± 80 Ma; the uppermost leucogabbros and quartz-gabbros have also been poorly dated at 719 ± 120 Ma, whereas late felsic pegmatoids have crystallized at 663 ± 8 Ma (U–Pb on zircons by ID-TIMS; data from H. de la Boisse, unpub. Ph.D. thesis, Univ. Montpellier 1979; recalculated following the method of Ludwig, 2003).

The descriptions and discussions below will only focus on various garnet occurrences and related structures and textures observed in the metagabbro unit and their relations to anorthositic veins and the anhydrous trondhjemite found in the upper part of the massif.

3. Analytical methods

Analyses of minerals were performed on the CAMECA SX50 and SX100 electron microprobes at CAMPARIS (University of Paris VI, France) and on a CAMECA SX50 microprobe at the CAMST (Université de Louvain-la-Neuve, Belgium). The operational conditions involve a current beam of 10 nA with an accelerating voltage of 15 keV. Counting time per element and background was fixed at 10 s. Standards used for calibration are natural and synthetic minerals.

Major elements on whole-rock samples were analysed by ICP-AES at the Musée Royal de l'Afrique Centale (Tervuren, Belgium). Rock powders were transformed into solution by alkaline fusion and were diluted in 5 % HNO_3. Seven international rock standards were used for calibration.

Trace elements were analysed by ICP-MS at the Musée Royal de l'Afrique Centrale. Powders were dissolved either by alkaline fusion (for samples with refractory minerals such as zircon or spinel), open acid digestion in Teflon® beakers or high-pressure acid digestion using Teflon® bombs (for samples with low trace element contents). Analyses were made on a VG PlasmaQuad 2+ spectrometer, and four artificial standards were used for external calibrations.

4. Styles of garnet occurrences in the Amalaoulaou metagabbros

Garnet is widespread in the metagabbros; it is commonly coarse-grained (up to 5 cm) and poikiloblastic with abundant inclusions. Several modes of occurrence can be distinguished on the basis of textural relationships between garnet and the anorthositic layers, veins or halos.

(1) Usually garnet is disseminated in the metagabbros as coarse poikiloblastic grains rich in clinopyroxene inclusions (~ 50 vol. %) and surrounded by a plagioclase-rich halo or tail (Figs 3a, b, 4a), depending on the degree of deformation. Each sample displays a micro-scale metamorphic differentiation with garnet–clinopyroxene-bearing microdomains surrounded by plagioclase-rich zones, whereas garnet-free domains show a homogeneous distribution of plagioclase and clinopyroxene (partly replaced by secondary amphibole). When comparing the modal proportion of this type of garnet metagabbros to surrounding garnet-free metagabbros that have the same chemical composition (see below), it appears that the garnet-bearing samples are enriched in clinopyroxene compared to garnet-free gabbros (54–56 vol. % instead of 37–44 vol. % in garnet-free domains; Fig. 5). Plagioclase proportions in the garnet-bearing domains are, however, lower than in the garnet-free metagabbro (25–26 and 53–59 vol. %, respectively).

(2) Garnet has also developed in direct association with anorthositic veins pre-dating the main metamorphic foliation. Coarse poikiloblastic garnet is then observed at the boundary between the host metagabbros and veins or within the veins (Fig. 3c, d). It is also characterized by numerous clinopyroxene inclusions. In the host metagabbros and close to the veins, coarse euhedral garnets are present and surrounded by a leucocratic halo (Fig. 3d), a structure that strongly resembles those observed in the partially melted Fiordland dioritic orthogneiss (Stevenson *et al.* 2005).

(3) Garnet also appears within leucocratic pockets found in the metagabbros (Fig. 3e). Again, this garnet is poikiloblastic with numerous clinopyroxene inclusions.

(4) Some leucocratic layers or veins associated with melanocratic garnet–clinopyroxene–rutile layers also contain coarse poikiloblastic garnet (Fig. 3f). In strongly deformed rocks, garnet–clinopyroxene–rutile rocks form boudins associated with coarse poikiloblastic garnets surrounded by plagioclase-dominant coronas (Fig. 3g).

(5) One sample (IC 936) has a migmatite-like structure (Fig. 3h) characterized by alternating

plagioclase-rich halo has developed close to the felsic vein; (e) garnet–plagioclase pocket in a metagabbro (hammer shaft is 40 mm across); (f) garnet–clinopyroxene–rutile layer (I) above a leucocratic layer containing coarse poikiloblastic garnets (leucosome, II); below these two layers, garnet metagabbros (III) overprint a former garnet-free metagabbro (IV); (g) deformed garnet-bearing felsic and ultramafic (Rst – restite) assemblages; note the absence of garnet away from the garnet–clinopyroxene–rutile restites and the coarse garnet-bearing leucocratic zones; (h) migmatitic-like metabasalt of melanocratic Grt–Cpx–Rt layers alternating with plagioclase-rich layers. A colour version of this figure can be viewed online at http://www.cambridge.org/journals/geo as Supplementary Material.

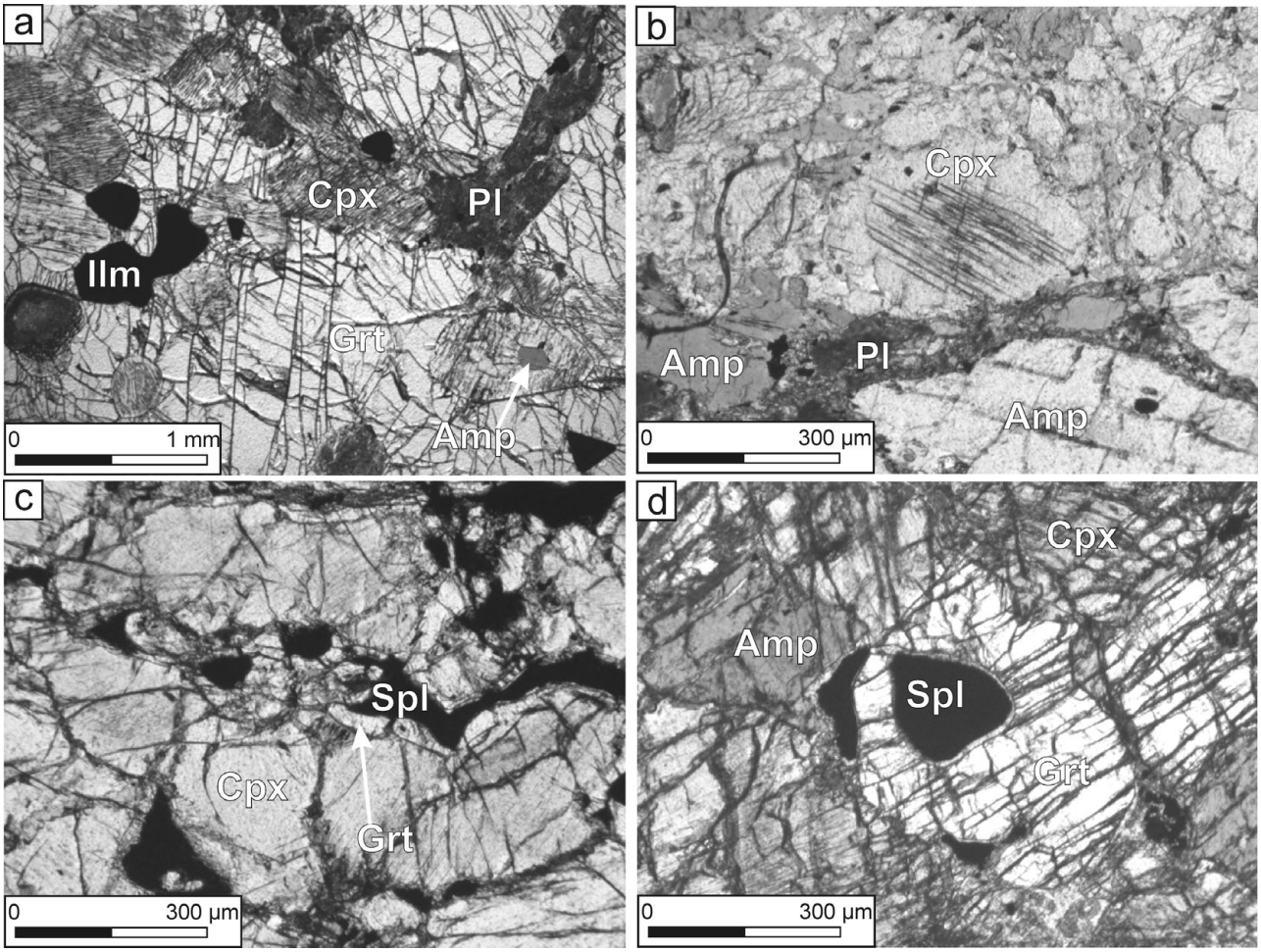

Figure 4. Microstructures in metagabbros and spinel pyroxenites. (a) Metagabbro AJB 2, coarse poikiloblastic garnet with clinopyroxene (Cpx), ilmenite (Ilm) and retrogressed plagioclase (Pl) inclusions; magmatic amphibole (Amp) is preserved as an inclusion into a clinopyroxene. (b) Clinopyroxene porphyroclast progressively replaced by recrystallized clinopyroxene and brown amphibole in metagabbro 04–73; plagioclase is totally retrogressed into fine-grained intergrowths of epidote and albite. (c) Garnet corona surrounding spinel in spinel pyroxenite AJB 29. (d) Coarse garnet with preserved spinel relic in a high temperature spinel and garnet pyroxenite (AJB 26). A colour version of this figure can be viewed online at http://www.cambridge.org/journals/geo as Supplementary Material.

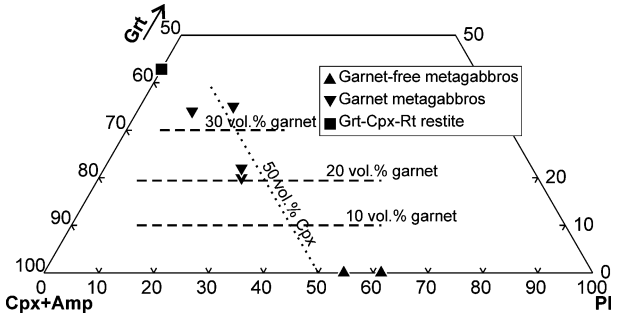

Figure 5. Garnet-free and garnet-bearing metagabbros showing large variation in modal compositions despite similar whole-rock geochemical compositions.

garnet–clinopyroxene–rutile layers (melanosomes) and anorthositic layers (leucosomes). Garnet is also present in the leucocratic layers but only at the contact between small melanocratic xenoliths and the anorthositic melt.

(6) One pyroxenite body cutting across the HT foliation of metagabbros shows the development of garnet porphyroblasts at the contact with the host metagabbro.

The modal composition of the inclusion assemblages found in the poikiloblastic garnets is the same for all the types described here. Garnet is rich in inclusions ($\sim$ 50 vol. % per garnet), among which clinopyroxene is by far the most abundant phase, even in the leucocratic gabbros. Plagioclase is very scarce (generally absent; $<$ 5 vol. % when present) and ilmenite is a common minor component (1–5 vol. %). Garnet development leads to the formation of ultramafic microdomains made of garnet–clinopyroxene–Fe–Ti oxide assemblages strongly depleted in plagioclase compared to the host rock.

The spinel and garnet pyroxenites have preserved evidence of the garnet-forming reaction. In most of the spinel pyroxenites, garnet forms a thin (20–100 μm) corona (Fig. 4c) between green aluminous spinel and clinopyroxene. In one sample (AJB 26), this coronitic texture progressively evolves to an equigranular texture with garnet in textural equilibrium with clinopyroxene,

but spinel is locally totally consumed or only present as rounded inclusions in the core of garnets (Fig. 4d).

5. Anorthositic veins and the trondhjemite

Two generations of anorthositic veins intrude the metagabbros. The first pre-dates the main metamorphic foliation and post-dates the magmatic fabric. These veins are generally folded but subconformable to the foliation underlined by secondary amphibole. Garnet is closely associated with these veins; it forms coarse poikiloblastic grains at the vein/host boundary or within the host metagabbros close to the contact with the veins. In some places partly preserved from the late deformation, garnet has clearly grown across a several-centimetre-thick reaction zone. The veins almost exclusively consist of totally retrogressed plagioclase (epidote + white mica + albite) with minor amounts of quartz (< 1 vol. %).

The second generation of veins is oblique to the main metamorphic foliation. Garnet is observed neither at the vein/host contact, nor within the veins. The latter have a strictly anorthositic modal composition, except for minor amounts of euhedral amphibole. Plagioclase is also totally retrogressed into secondary hydrous assemblages.

The trondhjemite considered in this paper consists of peculiar quartz–plagioclase assemblages characterized by the absence of mafic minerals (clinopyroxene, amphibole or biotite). Plagioclase (~ 45 vol. %) is also totally retrogressed into albite + epidote intergrowths (60 vol. % albite and 40 vol. % epidote with accessory pyrite) and the texture is medium-grained equigranular. Apatite is the only accessory phase (< 0.5 vol. %). Quartz (~ 55 vol. %) shows evidence for dynamic recrystallization, but the sample has preserved a macroscopic magmatic texture characterized by euhedral ghost plagioclase crystals.

6. Thermobarometry of garnet-bearing and garnet-free assemblages

6.a. Magmatic stage

One unzoned Ti-pargasite grain found as an inclusion within a clinopyroxene crystal from a garnet metagabbro (AJB 2) is considered to be of igneous origin. It has a different textural setting (Fig. 4a) relative to all secondary amphiboles replacing clinopyroxene, and it shows the highest titanium content recorded among all the amphiboles analysed for the Amalaoulaou massif (Appendix Table 1, available as supplementary material online at http://www.cambridge.org/journals/geo). Temperature and pressure of magmatic crystallization of metagabbros have been estimated at 950–1000 °C and 8–9 kbar with the Ti-in-amphibole thermometer of Féménias *et al.* (2006) and Al-in-hornblende barometer of Schmidt (1992). Clinopyroxene preserved from local equilibration with garnet and devoid of evidence of recrystallization (Cpx I) is the most Al-rich pyroxene (8–10 Al_2O_3 wt %, Appendix Table 2, available as supplementary material online at http://www.cambridge.org/journals/geo) and is probably of magmatic origin. The pressure of crystallization of this clinopyroxene has been estimated with the structural barometer of Nimis & Ulmer (1998). It gives a pressure of crystallization (9 kbar) similar to those calculated for the amphiboles.

6.b. Isobaric cooling

Triple junctions between coronitic garnet, orthopyroxene and clinopyroxene (Fig. 4c) in spinel pyroxenites allow determination of precise *P–T* conditions of formation. The rim of clinopyroxenes in contact with garnet always indicates lower non-quadrilateral element (Al, Ti, Na; Appendix Table 2, available as supplementary material online at http://www.cambridge.org/journals/geo) contents when compared to those found in the core of the grains (Al 0.27–0.33 a.p.f.u. and Mg no. 80–83 in the core; Al 0.15–0.29 a.p.f.u., Mg no. 83–87 at the rim), which means that local chemical equilibrium has been reached between garnet and pyroxene rims. By combining Grt–Cpx thermometry (Ganguly, 1979) with Grt–Opx thermobarometry (Harley, 1984*a*,*b*), the *P–T* conditions of coronitic garnet growth in the pyroxenites have been estimated at 700–750 °C for a pressure range of 7–8 kbar. The same temperatures (720–750 °C) have been estimated for the Opx–Cpx pair (Bertrand & Mercier, 1985) in a metagabbro in which both pyroxenes show local chemical equilibration evidenced by a decrease in non-quadrilateral element contents between core and rim (Al from 0.21 to 0.13 a.p.f.u. in opx and from 0.33 to 0.27 a.p.f.u. in Cpx, Appendix Table 2 and 3, available as supplementary material online at http://www.cambridge.org/journals/geo).

6.c. High temperature overprint

In one spinel pyroxenite (AJB 26), the garnet (Appendix Table 4, available as supplementary material online at http://www.cambridge.org/journals/geo) surrounding spinel has evolved to a porphyroblastic texture with spinel only present as relic rounded grains included within garnet (Fig. 4d). The Grt–Cpx equilibration temperatures are significantly higher than those estimated for the coronitic stage; they range from 810 to 910 °C for a pressure fixed at 10 kbar (no independent estimation of pressure can be made because orthopyroxene was not observed in this sample). High temperatures are also recorded by Grt–Cpx pairs in metagabbros. Rounded clinopyroxene inclusions (Al 0.21–0.32 a.p.f.u., Mg no. 69–77) within garnet clearly show clear distinct compositions relative to those of primary clinopyroxene porphyroclasts (Al > 0.33 a.p.f.u., Mg no. 65–70). This suggests chemical equilibrium between the clinopyroxene inclusions and host garnets. Grt–Cpx thermometry yields

temperatures of equilibration in the range 730–910 °C with most temperatures above 810 °C. It thus clearly shows that garnet growth in the metagabbros has been enhanced by a temperature increase. No pressure calculations are possible for these rocks, but from phase equilibria constraints and petrogenetic experimental studies (Pattison, 2003), it is known that garnet-free gabbros do react to garnet-bearing assemblages at $T > 825$ °C at $P \geq 10$ kbar. A summary of P–T estimates is presented in Appendix Table 5, available as supplementary material online at http://www.cambridge.org/journals/geo.

7. Metagabbros and trondhjemite geochemistry and their relationship with island-arc rocks

Major element analysis of metagabbros from the Amalaoulaou massif (Appendix Table 6, available as supplementary material online at http://www.cambridge.org/journals/geo) show that they have a restricted range of composition and a tholeiitic affinity (H. de la Boisse, unpub. Ph.D. thesis, Univ. Montpellier, 1979). They show low silica (45–47 wt %) and potassium contents with high alumina content (15–20 wt %) for a Mg no. ranging between 50 and 60. The rare earth element patterns show LREE depletion with a slight convex-upward distribution ($(La/Sm)_N$ 0.5–1; $(Gd/Yb)_N$ 1.2–1.5) and no Eu anomaly despite the high modal proportion of retrogressed plagioclase. This profile is close to those of N-MORBs except for a relative depletion in HREE. Very similar patterns have been observed for tholeiites formed during the immature stage of the Caribbean intra-oceanic arc build-up (Fig. 6a). The multi-element pattern of the metagabbros (normalized to N-MORB) shows enrichment in Rb, K and Ba compared to MORBs, but generally lower contents in most HFSE (Zr, Ti, Y, HREE). Positive anomalies are observed for K, Ba, Sr and Pb and slight negative anomalies for Nb–Ta and Zr–Hf. The profile is parallel to that for the Kohistan garnet granulites but the Amalaoulaou metagabbros have generally higher trace element contents. A very similar pattern has been observed for the first generation of magmas from the Caribbean island arc (Fig. 6b). In a Sr/Y v. $(La/Sm)_N$ diagram (Fig. 7), the metagabbros have a Sr/Y ratio significantly higher than in Atlantic N-MORBs; they plot within the field of intra-oceanic arc lavas (exemplified by Caribbean Cretaceous lava) rather than in the continental Andean-type lavas field. The latter are indeed characterized by $(La/Sm)_N$ ratios higher than 1, whereas LREE depletion is a common feature of island-arc tholeiites.

The trondhjemite described above has high silica (77 wt %), low K (0.88 K_2O wt %) and low $Fe_2O_3t + MgO + TiO_2$ contents (< 1 wt %) in agreement with its mineralogy. The trace element pattern is remarkable, being strongly depleted in HREE ($(La/Yb)_N$ 157 instead of 1.0–1.2 for the metagabbros), but also for its extremely low contents of Y, Ti, Zr and Hf (Fig. 6b). The strong depletion in HREE and

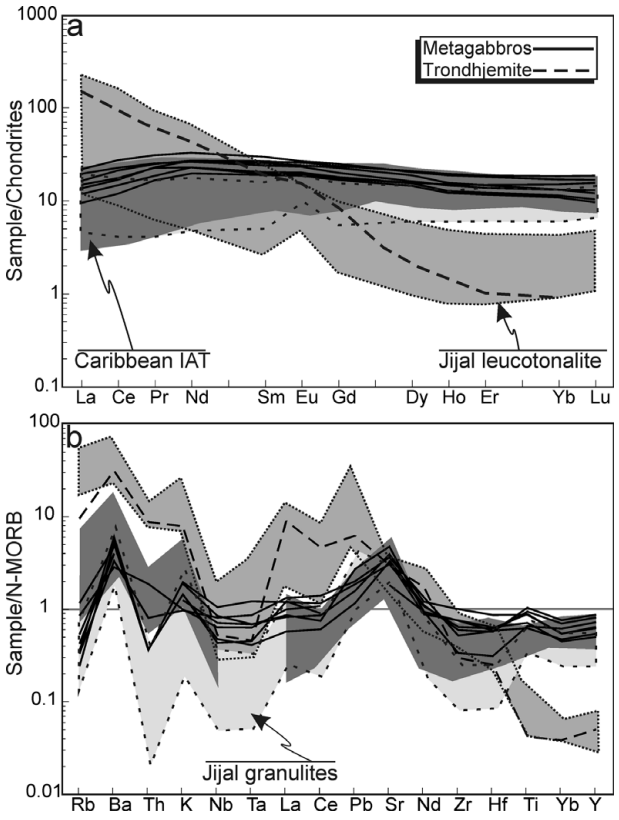

Figure 6. (a) REE patterns of metagabbros and trondhjemite from the Amalaoulaou massif compared to oceanic arc rocks; normalization values from McDonough & Sun (1995). (b) Multi-element diagram showing the composition of the Amalaoulaou metagabbros and trondhjemite; Jijal metagabbros and tonalites from the Kohistan complex from Garrido *et al.* (2006); Cretaceous island-arc tholeiites from the Caribbean (Escuder-Viruete *et al.* 2006); N-MORB values from Hofmann (1988).

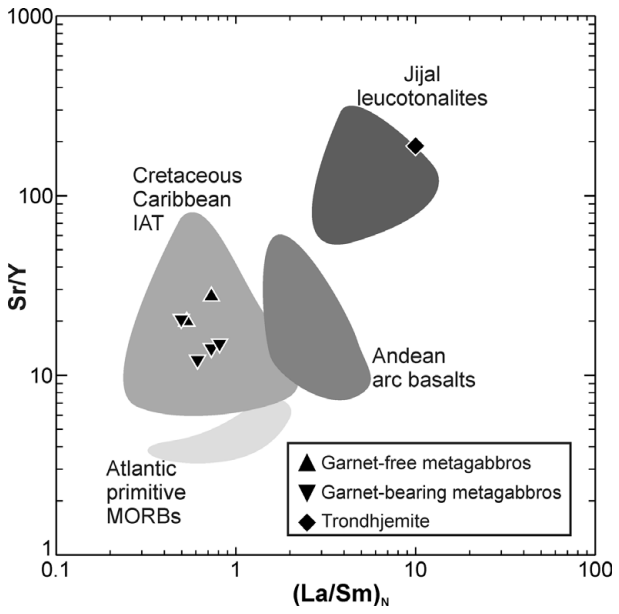

Figure 7. Sr/Y v. $(La/Sm)_N$ diagram for the Amalaoulaou metagabbros and the trondhjemite. For comparison: Atlantic primitive MORBs (Klein, 2003); Cretaceous island-arc tholeiites from the Caribbean (Escuder-Viruete *et al.* 2006); basalts from the continental Andean arc (130 analyses from the online GEOROC database) and Jijal leucotonalites formed by dehydration melting of garnet granulites in the Kohistan island-arc root (from Garrido *et al.* 2006).

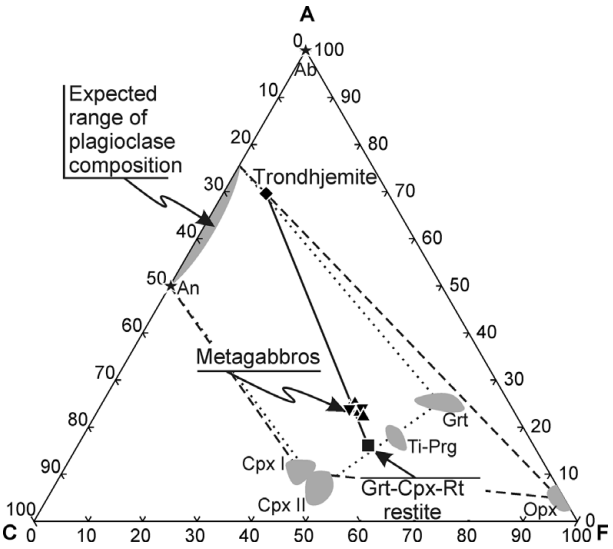

Figure 8. Molar ACF ($A – Al_2O_3$, C – CaO, $F – FeO_{tot}$+MgO) diagram for garnet-free and garnet-bearing metagabbros, garnet–clinopyroxene–rutile melanosomes, trondhjemite and constitutive minerals. The grey shaded area along the A–C join shows the expected compositional range of plagioclase from the metagabbros, as inferred from the range in bulk composition of the epidote–albite intergrowths replacing this plagioclase.

Y suggests that garnet has played an important role in the genesis of this trondhjemite (garnet fractionation or melting of a garnet-bearing residue) and the depletion in Ti, Zr and Hf suggests that rutile and/or ilmenite either was fractionated or was part of the partial melting residue. The trondhjemite plots within the field of the leucotonalites from the Jijal section of the Kohistan oceanic arc in a Sr/Y v. $(La/Sm)_N$ diagram. All the geochemical similarities shared by the Amalaoulaou trondhjemite and the leucotonalites from Kohistan suggest a similar mode of formation. In an ACF diagram (Fig. 8), the metagabbros plot on a line joining the trondhjemite and the garnet–clinopyroxene–rutile melanosome. A simple mass balance calculation shows that by adding 15 vol. % of trondhjemite to 85 vol. % of the ultramafic assemblage, a composition very close to the metagabbro is obtained. The metagabbros are probably the source of the trondhjemitic melt, and the garnet–clinopyroxene–rutile assemblage most probably represents the restite after melting. Similar conclusions have been drawn for the genesis of the Jijal leucotonalites in the root of the Kohistan oceanic arc (Garrido *et al.* 2006).

The Amalaoulaou metagabbros and the trondhjemite are thus characterized by geochemical signatures that are typically encountered in island-arc series. Moreover, the absence of continental rocks within the massif and the absence of K- and Al-rich lithologies (both observed within the continental arcs present along the same suture zone: Liégeois, Bertrand & Black, 1987; Duclaux *et al.* 2006) strongly suggest that the Amalaoulaou basic–ultrabasic massif has been formed in a intra-oceanic setting above a subducting oceanic slab.

8. Discussion

8.a. Origin of garnet in the Amalaoulaou arc root

Several mechanisms are possible to explain garnet growth in the metagabbros and the pyroxenites: solid-state garnet growth in response to a pressure increase or a cooling event; dehydration reactions involving the breakdown of hornblende into anhydrous, garnet-bearing assemblages; peritectic growth of garnet related to melting and magmatic crystallization of garnet. These hypotheses are discussed in the next sections.

8.a.1. Solid-state garnet-forming reaction

The transition from garnet-free to garnet-bearing granulites is a univariant curve with a positive slope in *P–T* space (Green & Ringwood, 1967). Garnet growth can thus be induced either by a pressure increase or a temperature decrease. Such reactions classically involve an aluminous phase (plagioclase, spinel) and a ferromagnesian silicate (pyroxene). In the spinel pyroxenites from Amalaoulaou, the coronitic textural setting of garnet indicates that it has grown at the expense of spinel and pyroxenes, a classical garnet-forming reaction in pyroxenites.

In the metagabbros where spinel is absent, there is no textural evidence for a reaction between pyroxenes and plagioclase to form garnet, as is the case in deep-seated granulitic xenoliths (Berger *et al.* 2005). In the Amalaoulaou metagabbros, garnet is indeed euhedral and coarse-grained, and occurs in leucocratic as well as in melanocratic layers. Moreover, in the absence of aluminous spinel in metagabbros, the only reaction which could produce garnet involves a breakdown of plagioclase and pyroxene. The garnet metagabbros have a higher modal proportion of clinopyroxene than the garnet-free metagabbros, although the two rock types have the same whole-rock composition. Reactions involving orthopyroxene and plagioclase to form garnet and clinopyroxene are also described from exposed massif in Hoggar (Mokri *et al.* 2008). However, at Amalaoulaou, orthopyroxene is locally observed close to coarse garnet porphyroblasts and it does not show the development of coronitic garnet at the contact with former plagioclase. These observations exclude the hypothesis according to which garnet would have formed by a solid-state, vapour-absent reaction in the metagabbros.

8.a.2. Dehydration and dehydration melting

Dehydration and dehydration melting reactions are characterized by the breakdown of a hydrous phase into an anhydrous assemblage. In mafic rocks, amphibole is the most common hydrous mineral and, in response to a temperature increase, it can break down into garnet–clinopyroxene or two-pyroxene assemblages, depending on the pressure (see references in Pattinson, 2003). These reactions are also plagioclase-consuming and clinopyroxene-producing. This agrees with the

evolution of the modal proportion in metagabbros where the presence of garnet is linked to an increase in clinopyroxene/plagioclase modal ratio. Garnet is coarse-grained in most of the garnet metagabbros (up to 5 cm in diameter); in most dehydration experiments as well as in natural examples of dehydration, garnet is also generally coarser than the coexisting phases. This is most probably linked to the presence of water during garnet growth, which has the effect of increasing growth rates during the dehydration reactions (Rushmer, 1993; Wolf & Wyllie, 1993).

The close relationship between early anorthositic veins and the presence of coarse garnets in the host metagabbros has been observed in other arc roots and is best documented in the Fiordland massif (Daczko, Clarke & Klepeis, 2001) and in the Jijal complex of Kohistan (Burg *et al.* 1998; Yamamoto & Yoshino, 1998; Garrido *et al.* 2006). Garnet growth has been ascribed to the breakdown of amphibole into anhydrous garnet-bearing assemblages in response to heat increase caused by anorthosite-vein intrusions. These transformations are virtually isochemical except for the alkalis (Yamamoto & Yoshino, 1998). The temperatures recorded by the garnet–clinopyroxene pairs in the Amalaoulaou metagabbros (730–900 °C with most $T > 810$ °C) are close to those determined for the dehydration reaction curves (isotherm close to 850 °C: Pattinson, 2003); the metagabbros have thus recorded *P–T* conditions that may have enhanced amphibole dehydration reactions.

Dehydration melting reactions are based on the same mechanisms as those in dehydration reactions, except that the reaction products comprise a felsic melt instead of water. Some migmatitic structures found in Amalaoulaou as well as the numerous felsic veins intruding the metagabbroic sequence are evidence for melting in the deep arc crust. Mass balance calculations show that the composition of a mixture of felsic melt and garnet–clinopyroxene–rutile restite in the proportion 15:85 matches the composition of the metagabbroic protolith. Numerous experimental studies show that garnet–clinopyroxene–rutile rocks are restites of a melted metabasite around 10 kbar and that the melt produced ranges from anorthositic to tonalitic (see Section 8.b). The local, small-scale, metamorphic differentiation of the metagabbros into clinopyroxene-rich poikiloblastic garnets surrounded by plagioclase halos strongly suggests that melting has affected most of the garnet-bearing metagabbros, but that the resulting melt was not extracted from the overall melting zone because whole-rock compositions of garnet-bearing and garnet-free samples are identical. This texture is comparable to that induced by the formation of peritectic garnets in the Fiordland mafic orthogneiss (Stevenson *et al.* 2005). The transformation of two-pyroxene granulites into garnet-bearing granulites in Mesozoic arc roots has also been explained by dehydration and dehydration melting (Daczko, Clarke & Klepeis, 2001; Garrido *et al.* 2006).

Magmatic amphibole is not easy to identify in the Amalaoulaou metagabbros because this phase has been strongly retrogressed under transitional upper amphibolite/granulite facies conditions. This is shown by the ubiquitous development of brown amphibole as a replacement product of clinopyroxene. Several arguments, however, strongly support the presence of magmatic pargasite: (1) brown Ti-pargasite has been found as inclusions within a granulitic clinopyroxene, suggesting that it was present before granulite-facies equilibration and concomitant garnet growth. This amphibole has the highest Ti content relative to all the other secondary amphiboles in Amalaoulaou; (2) large amphibole grains sometimes show sharp contacts with clinopyroxene, which contrasts with the clinopyroxene replacement textures characteristic of the secondary amphibole; however, this supposedly primary amphibole has planar rutile exsolutions which makes its original composition relatively unsure; (3) magmatic brown pargasite is a common major-to-accessory phase in deep enriched subalkaline mafic rocks (Foden & Green, 1992; Hermann, Müntener & Gunther, 2001; Desmurs, Müntener & Manatschal, 2002) and monomineralic amphibole cumulates (hornblendites) are commonly found in arc roots (Garrido *et al.* 2006).

8.a.3. Magmatic crystallization

Garnet can crystallize from calc-alkaline melts of intermediate to acid composition (see Harangi *et al.* 2001), but only at pressures exceeding 8 kbar. The garnet effect is generally clearly imprinted in the geochemical signature: whole-rock compositions are enriched in HREE and Y whenever garnet is a cumulus phase, while the melts show a depletion in these elements in response to garnet fractionation. As no samples with intermediate compositions between garnet metagabbros and trondhjemites have been found, it is difficult to link these two rock types by fractional crystallization of garnet-bearing cumulates. The magmatic origin of garnet is thus excluded at Amalaoulaou.

8.b. Generation of melts in a deep Neoproterozoic arc crust

The anorthositic veins observed in the metagabbroic sequence can be ascribed to two distinct generations distinguished by their mineralogy as well as by their time of emplacement. The earliest is characterized by conspicuous garnet at the vein/host boundaries and pre-dates the main metamorphic foliation. The second has no garnet at the host/vein contacts and distinctly cuts across this metamorphic foliation. Garnet–clinopyroxene temperatures for poikiloblastic garnets surrounded by plagioclase-rich halos are close to those at the dehydration-melting solidus, 850 °C. Indeed, Selbekk & Skjerlie (2002) have experimentally obtained anorthositic melts with garnet-bearing mafic residues at pressures above 10 kbar for temperatures

between 800 and 1000 °C. However, the melting conditions in these experiments were controlled by high H_2O contents, which stabilize amphibole in the residue and in the melts. In the Amalaoulaou metagabbros, the generation of anorthositic melts (containing scarce amphibole) is accompanied by the production of garnet and clinopyroxene, with no residual amphibole in equilibrium with garnet.

The trondhjemites strongly depleted in HREE, Y, Ti, Zr and Hf are probably the result of gabbro melting in the Amalaoulaou arc root. Indeed, the peculiar geochemical fingerprint cannot be explained by fractionation of garnet from evolved mantle-derived melts for two main reasons: (1) the trondhjemite is clearly younger than all the other lithologies, as the trondhjemitic and tonalitic stocks cut across the quartz gabbros and (2) none of the analysed samples have an intermediate composition between those of the trondhjemite and the mafic rocks (quartz gabbros and metagabbros). Tonalitic and trondhjemitic melts are easily produced experimentally by dehydration melting of deep mafic rocks (Beard & Lofgren, 1991; Wolf & Wyllie, 1991; Sen & Dunn, 1994; Rapp & Watson, 1995; Lopez & Castro, 2001) and are also observed in nature (Garrido *et al.* 2006). All these authors show that the residues in equilibrium with trondhjemites are dominated by clinopyroxene, garnet and rutile, and these associations are observed either as small boudins in the metagabbro unit or in the melanosomes of the migmatitic bodies at Amalaoulaou. The trondhjemitic melts have been formed from a garnet-and-rutile-bearing restitic source that is, using the geochemical arguments cited above, from the garnet–clinopyroxene–rutile assemblages locally preserved as layers or boundins within the metagabbros. Rapp & Watson (1995) have shown that a very similar rock can be formed by partial melting of a metabasalt with a composition close to those of the Amalaoulaou metagabbros. The *P–T* conditions for trondhjemitic melt formation in these experiments is between 1050 and 1100 °C (above the amphibole-out reaction curve in the restite) for pressures above 10 kbar and melting ratios between 20 and 40 %).

The combination of the thermobarometric results and the experimental data leads us to consider that the production of anorthosite melt from metagabbro melting occurred at near-solidus temperatures (~ 850 °C) in slightly hydrous conditions (< 1 wt % H_2O) and at pressures probably around 10 kbar. The primary amphibole was present in minor proportions in the metagabbros (< 15 vol. %) and it was rapidly consumed during the early stage of melting. From experimental data, the trondhjemites are most probably higher-temperature melts (1050–1100 °C) formed at $P > 10$ kbar. The anhydrous nature of the trondhjemite and of the equilibrium restite means that an independent water phase was no longer present during trondhjemite formation; it is thus inferred that primary amphibole was totally consumed at this stage of melting.

8.c. Isobaric cooling followed by maturation of the arc

Garnet-free metagabbros, characterized by relic plagioclase–clinopyroxene–orthopyroxene–amphibole assemblages, yield two-pyroxene equilibration temperatures of 720–750 °C. Most temperatures given by clinopyroxene–garnet pairs in the garnet metagabbros are above 810 °C and up to 900 °C. The presence of garnet at these temperatures suggests pressures exceeding 10 kbar, whereas garnet-free assemblages are usually ascribed to pressures below 10 kbar (Pattinson, 2003). The spinel and garnet pyroxenites show the same *P–T* evolution: the coronitic-garnet stage is characterized by equilibrium conditions of 700–750 °C/7–8 kbar, followed by a more pronounced development of garnet toward an equant texture developed at 800–900 °C (Appendix Table 5, available as supplementary material online at http://www.cambridge.org/journals/geo). We can thus propose that the magmatic gabbros and pyroxenites have crystallized at high temperatures and pressures (from amphibole thermometry), ~ 950 °C/8–9 kbar (stage A), and have cooled down to 700–750 °C/7–9 kbar (stage B). Subsequently, these two main lithologies have undergone a pressure and temperature increase that has induced formation of garnet in the metagabbros and locally enhanced melting (up to 1050 °C and $P \geq 10$ kbar, stages C and D).

Such events marked by a pressure and temperature increase (Fig. 9) in static conditions are common in arc roots and probably reflect the arc maturation (growth) by magma intrusion at shallower depth and

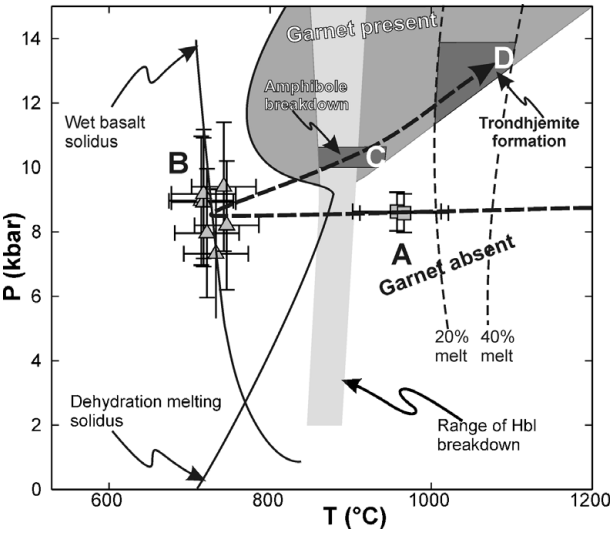

Figure 9. *P–T* evolution and proposed path for the magmatic and granulitic evolution of the Amalaoulaou metagabbros. Dehydration-melting solidus of hydrous, hornblende-bearing metabasalt and garnet-present/garnet-absent domains from Lopez & Castro (2001); wet solidus from Vielzeuf & Schmidt (2001); curves labelled 20 vol. % and 40 vol. % melt represent the *P–T* conditions where respectively 20 and 40 vol. % of felsic melt were present during partial melting experiments on hydrous metabasalts (from Rapp & Watson, 1995); *P–T* range for hornblende breakdown from Pattinson (2003). A, B, C and D represent the four evolution stages described in the text.

burial of the underlying units, including the deep arc root (Kelemen, Hanghoj & Greene, 2003; Garrido *et al.* 2006). The hot geotherm required to cross the dehydration-melting solidus can be reached by arc root burial in an environment where underplating of mantle-derived magmas (basalt and high-Mg andesites) at the base of arc crust can bring enough heat to maintain high temperatures. Direct intrusion and impregnation of melt within the arc lower crust are also in part responsible for garnet growth. Coarse garnets are indeed observed at the contact with anorthosite veins and sometimes in a thin rim surrounding pyroxenite bodies that cut across the foliation of the metagabbros. These features are generally interpreted as small-scale contact metamorphism between vein and host (Yamamoto & Yoshino, 1998; Daczko, Clarke & Klepeis, 2001; Garrido *et al.* 2006) and reflect impregnation of metagabbros by melts derived either from partial melting of the arc lower crust (anorthosite/trondhjemite) or of the mantle (pyroxenites).

The melting and dehydration event at Amalaoulaou has locally generated garnet granulites and garnet–clinopyroxene–rutile restites whose density can reach 3.5 g/cm^3 at 20 % melting (Wolf & Wyllie, 1993). If large volumes of restites are formed with densities greater than that of the underlying mantle, the density contrast could induce gravitational instability (Jull & Kelemen, 2001). Foundering of dense ultramafic restites (also refered as delamination) can thus be a mechanism driving the composition of the arcs from basaltic to andesitic and is one of the solutions proposed to solve the 'arc paradox' of continental crust formation. Through this process, the melting event generates tonalites depleted in K–Ti–Fe–Mn–Mg that closely match the composition of those in tonalite–trondhjemite–granodiorite (TTG) suites (Martin *et al.* 2005). The Amalaoulaou island-arc root thus represents a crucial geological object that may aid in understanding the mechanisms of continental crust formation, because it shows the association of ultramafic, garnet-bearing dense restite with felsic melts resembling those from TTG suites observed in Precambrian cratons.

Acknowledgements. JB and RC sincerely thank all the participants and the organizers of the IGCP 485 meeting 2006 in Gourma for fruitful discussions and for providing some photographs. F. Buscail has provided helpful GIS data of the Gourma geological map. B. Dhuime and D. Bosch shared their samples from Amalaoulaou and most of these were helpful for understanding melting processes in the arc root. Finally, we have appreciated the comments and suggestions of the two anonymous reviewers which led to significant improvements of the manuscript, and the editorial handling of D. M. Pyle and J. Holland is gratefully acknowledged.

References

BARD, J. P., MALUSKI, H., MATTE, P. & PROUST, F. 1980. The Kohistan sequence; crust and mantle of an obducted island arc. *Geological Bulletin, University of Peshawar* **13**, 87–93.

BAYER, R. & LESQUER, A. 1978. Les anomalies gravimétriques de la bordure orientale du craton ouest-africain: géométrie d'une suture panafricaine. *Bulletin de la Société Géologique de France* **20**, 863–76.

BEARD, J. S. & LOFGREN, G. E. 1991. Dehydration melting and water-saturated melting of basaltic and andesitic greenstones and amphibolites at 1, 3, and 6.9 kb. *Journal of Petrology* **32**, 365–401.

BEHN, M. D. & KELEMEN, P. B. 2006. Stability of arc lower crust: Insights from the Talkeetna arc section, south central Alaska, and the seismic structure of modern arcs. *Journal of Geophysical Research – Solid Earth* **111** (B11207), doi:10.1029/2006JB004327, 20 pp.

BERGER, J., FÉMÉNIAS, O., COUSSAERT, N. & DEMAIFFE, D. 2005. Magmatic garnet-bearing mafic xenoliths (Puy Beaunit, French Massif Central): P–T path from crystallization to exhumation. *European Journal of Mineralogy* **17**, 687–701.

BERTRAND, P. & MERCIER, J.-C. C. 1985. The mutual solubility of coexisting ortho- and clinopyroxene; toward an absolute geothermometer for the natural system? *Earth and Planetary Science Letters* **76**, 109–22.

BLACK, R., LATOUCHE, L., LIÉGEOIS, J. P., CABY, R. & BERTRAND, J. M. 1994. Pan-African displaced terranes in the Tuareg shield (central Sahara). *Geology* **22**, 641–4.

BRADSHAW, J. Y. 1989. Origin and metamorphic history of an Early Cretaceous polybaric granulite terrain, Fiordland, Southwest New Zealand. *Contributions to Mineralogy and Petrology* **103**, 346–60.

BURG, J. P., BODINIER, J. L., CHAUDHRY, S., HUSSAIN, S. & DAWOOD, H. 1998. Infra-arc mantle–crust transition and intra-arc mantle diapirs in the Kohistan Complex (Pakistani Himalaya): petro-structural evidence. *Terra Nova* **10**, 74–80.

CABY, R. 1979. Les nappes précambriennes du Gourma dans la chaîne pan-africaine du Mali. *Revue de Géologie Dynamique et de Géographie Physique* **21**, 367–76.

CABY, R. 1994. Precambrian coesite from Northern Mali – First record and implications for plate-tectonics in the Trans-Saharan segment of the Pan-African belt. *European Journal of Mineralogy* **6**, 235–44.

CABY, R., ANDREOPOULOS-RENAUD, U. & PIN, C. 1989. Late Proterozoic arc–continent and continent–continent collision in the Pan-African Trans-Saharan Belt of Mali. *Canadian Journal of Earth Sciences* **26**, 1136–46.

CABY, R., BUSCAIL, F., DEMBELE, D., DIAKITE, S., SACKO, S. & BALL, M. 2008. Neoproterozoic garnet-glaucophanites and eclogites: new insights for subduction metamorphism of the Gourma fold-and-thrust belt (eastern Mali). In *The boundaries of the West African Craton* (eds N. Ennih & J.-P. Liégeois), pp. 203–16. Geological Society of London, Special Publication no. 297.

DACZKO, N. R., CLARKE, G. L. & KLEPEIS, K. A. 2001. Transformation of two-pyroxene hornblende granulite to garnet granulite involving simultaneous melting and fracturing of the lower crust, Fiordland, New Zealand. *Journal of Metamorphic Geology* **19**, 547–60.

DEBARI, S. M. & COLEMAN, R. G. 1989. Examination of the deep levels of an island-arc – Evidence from the Tonsina ultramafic–mafic assemblage, Tonsina, Alaska. *Journal of Geophysical Research – Solid Earth and Planets* **94**, 4373–91.

DESMURS, L., MÜNTENER, O. & MANATSCHAL, G. 2002. Onset of magmatic accretion within a magma-poor rifted margin: a case study from the Platta

ocean–continent transition, eastern Switzerland. *Contributions to Mineralogy and Petrology* **144**, 365–82.

DOSTAL, J., DUPUY, C. & CABY, R. 1994. Geochemistry of the Neoproterozoic Tilemsi belt of Iforas (Mali, Sahara) – a crustal section of an oceanic island-arc. *Precambrian Research* **65**, 55–69.

DOSTAL, J., CABY, R., DUPUY, C., MEVEL, C. & OWEN, J. V. 1996. Inception and demise of a Neoproterozoic ocean basin: Evidence from the Ougda complex, western Hoggar (Algeria). *Geologische Rundschau* **85**, 619–31.

DUCLAUX, G., MENOT, R. P., GUILLOT, S., AGBOSSOUMONDÉ, Y. & HILAIRET, N. 2006. The mafic layered complex of the Kabye massif (north Togo and north Benin): Evidence of a Pan-African granulitic continental arc root. *Precambrian Research* **151**, 101–18.

ESCUDER-VIRUETE, J., DE NEIRA, A. D., HUERTA, P. P. H., MONTHEL, J., SENZ, J. G., JOUBERT, M., LOPERA, E., ULLRICH, T., FRIEDMAN, R., MORTENSEN, J. & PEREZ-ESTAUN, A. 2006. Magmatic relationships and ages of Caribbean Island arc tholeiites, boninites and related felsic rocks, Dominican Republic. *Lithos* **90**, 161–86.

FÉMÉNIAS, O., MERCIER, J. C. C., NKONO, C., DIOT, H., BERZA, T., TATU, M. & DEMAIFFE, D. 2006. Calcic amphibole growth and compositions in calc-alkaline magmas: Evidence from the Motru Dike Swarm (Southern Carpathians, Romania). *American Mineralogist* **91**, 73–81.

FODEN, J. D. & GREEN, D. H. 1992. Possible role of amphibole in the origin of andesite – some experimental and natural evidence. *Contributions to Mineralogy and Petrology* **109**, 479–93.

GANGULY, J. 1979. Garnet and clinopyroxene solid solutions, and geothermometry based on Fe–Mg distribution coefficient. *Geochimica et Cosmochimica Acta* **43**, 1021–9.

GARRIDO, C. J., BODINIER, J. L., BURG, J. P., ZEILINGER, G., HUSSAIN, S. S., DAWOOD, H., CHAUDHRY, M. N. & GERVILLA, F. 2006. Petrogenesis of mafic garnet granulites in the lower crust of the Kohistan palaeo-arc complex (Northern Pakistan): Implications for intra-crustal differentiation of island arcs and generation of continental crust. *Journal of Petrology* **47**, 1873–1914.

GREEN, D. H. & RINGWOOD, A. E. 1967. An experimental investigation of the gabbro to eclogite transformation and its petrological applications. *Geochimica et Cosmochimica Acta* **31**, 767–833.

GREENE, A. R., DEBARI, S. M., KELEMEN, P. B., BLUSZTAJN, J. & CLIFT, P. D. 2006. A detailed geochemical study of island arc crust: the Talkeetna Arc section, south-central Alaska. *Journal of Petrology* **47**, 1051–93.

HARANGI, S., DOWNES, H., KOSA, L., SZABO, C., THIRLWALL, M. F., MASON, P. R. D. & MATTEY, D. 2001. Almandine garnet in calc-alkaline volcanic rocks of the northern Pannonian Basin (eastern-central Europe): Geochemistry, petrogenesis and geodynamic implications. *Journal of Petrology* **42**, 1813–43.

HARLEY, S. L. 1984*a*. The solubility of alumina in orthopyroxene coexisting with garnet in FeO–MgO–Al_2O_3–SiO_2 and CaO–FeO–MgO–Al_2O_3–SiO_2. *Journal of Petrology* **25**, 665–96.

HARLEY, S. L. 1984*b*. An experimental study of the partitioning of Fe and Mg between garnet and orthopyroxene. *Contributions to Mineralogy and Petrology* **86**, 359–73.

HERMANN, J., MÜNTENER, O. & GUNTHER, D. 2001. Differentiation of mafic magma in a continental crust-to-mantle transition zone. *Journal of Petrology* **42**, 189–206.

HOFMANN, A. W. 1988. Chemical differentiation of the Earth – the relationship between mantle, continental-crust, and oceanic-crust. *Earth and Planetary Science Letters* **90**, 297–314.

HOLLIS, J. A., CLARKE, G. L., KLEPEIS, K. A., DACZKO, N. R. & IRELAND, T. R. 2003. Geochronology and geochemistry of high-pressure granulites of the Arthur River Complex, Fiordland, New Zealand: Cretaceous magmatism and metamorphism on the palaeo-Pacific Margin. *Journal of Metamorphic Geology* **21**, 299–313.

JAHN, B., CABY, R. & MONIÉ, P. 2001. The oldest UHP eclogites of the World: age of UHP metamorphism, nature of protoliths and tectonic implications. *Chemical Geology* **178**, 143–58.

JULL, M. & KELEMEN, P. B. 2001. On the conditions for lower crustal convective instability. *Journal of Geophysical Research – Solid Earth* **106**, 6423–46.

KAY, R. W. & KAY, S. M. 1988. Crustal recycling and the Aleutian arc. *Geochimica et Cosmochimica Acta* **52**, 1351–9.

KELEMEN, P. B., HANGHOJ, K. & GREENE, A. R. 2003. One view of the geochemistry of subduction-related magmatic arcs, with emphasis on primitive andesite and lower crust. In *Treatise on geochemistry vol. 3: The Crust* (ed R. L. Rudnick), pp. 593–659. Oxford: Elsevier-Pergamon.

KLEIN, E. M. 2003. Geochemistry of the igneous oceanic crust. In *Treatise on geochemistry vol. 3: The Crust* (ed. R. L. Rudnick), pp. 433–63. Oxford: Elsevier-Pergamon.

KODAIRA, S., SATO, T., TAKAHASHI, N., MIURA, S., TAMURA, Y., TATSUMI, Y. & KANEDA, Y. 2007. New seismological constraints on growth of continental crust in the Izu-Bonin intra-oceanic arc. *Geology* **35**, 1031–4.

LIÉGEOIS, J. P., BERTRAND, J. M. & BLACK, R. 1987. The subduction- and collision-related Pan-African composite batholith of the Adrar des Iforas (Mali); a review. *Geological Journal* **22**, 185–211.

LOPEZ, S. & CASTRO, A. 2001. Determination of the fluid-absent solidus and supersolidus phase relationships of MORB-derived amphibolites in the range 4–14 kbar. *American Mineralogist* **86**, 1396–1403.

LUDWIG, K. R. 2003. *User's manual for Isoplot 3.00. A geochronological toolkit for Microsoft Excel*. Berkeley Geochronology Center, Special Publication no. 4a.

MARTIN, H., SMITHIES, R. H., RAPP, R., MOYEN, J. F. & CHAMPION, D. 2005. An overview of adakite, tonalite–trondhjemite–granodiorite (TTG), and sanukitoid: relationships and some implications for crustal evolution. *Lithos* **79**, 1–24.

MATTINSON, J. M., KIMBROUGH, D. L. & BRADSHAW, J. Y. 1986. Western Fiordland orthogneiss; Early Cretaceous arc magmatism and granulite facies metamorphism, New Zealand. *Contributions to Mineralogy and Petrology* **92**, 383–92.

MCDONOUGH, W. F. & SUN, S. S. 1995. The Composition of the Earth. *Chemical Geology* **120**, 223–53.

MOKRI, M., OUZEGANE, K., KIENAST, J. R. & CABY, R. 2008. Evolution pression et température des métagabbros à grenat du complexe du camp Zora (terrane de l'Ahnet, Nord-Ouest du Hoggar). *Bulletin du Service Géologique de l'Algérie* **19**, 17–31.

MÜNTENER, O. & ULMER, P. 2006. Experimentally derived high-pressure cumulates from hydrous arc magmas and consequences for the seismic velocity structure of lower arc crust. *Geophysical Research Letters* **33**, L21308.

NIMIS, P. & ULMER, P. 1998. Clinopyroxene geobarometry of magmatic rocks Part 1: An expanded structural geobarometer for anhydrous and hydrous, basic and

ultrabasic systems. *Contributions to Mineralogy and Petrology* **133**, 122–35.

PATTINSON, D. R. M. 2003. Petrogenetic significance of orthopyroxene-free garnet plus clinopyroxene plus plagioclase +/− quartz-bearing metabasites with respect to the amphibolite and granulite facies. *Journal of Metamorphic Geology* **21**, 21–34.

RAPP, R. P. & WATSON, E. B. 1995. Dehydration melting of metabasalt at 8–32 kbar – Implications for continental growth and crust–mantle recycling. *Journal of Petrology* **36**, 891–931.

RINGUETTE, L., MARTIGNOLE, J. & WINDLEY, B. F. 1999. Magmatic crystallization, isobaric cooling, and decompression of the garnet-bearing assemblages of the Jijal Sequence (Kohistan Terrane, western Himalayas). *Geology* **27**, 139–42.

RUDNICK, R. L. 1995. Making continental crust. *Nature* **378**, 571–8.

RUSHMER, T. 1993. Experimental high-pressure granulites – Some applications to natural mafic xenolith suites and Archaean granulite terranes. *Geology* **21**, 411–14.

SCHMIDT, M. W. 1992. Amphibole composition in tonalite as a function of pressure – an experimental calibration of the Al-in-hornblende barometer. *Contributions to Mineralogy and Petrology* **110**, 304–10.

SELBEKK, R. S. & SKJERLIE, K. P. 2002. Petrogenesis of the anorthosite dyke swarm of Tromso, North Norway: Experimental evidence for hydrous anatexis of an alkaline mafic complex. *Journal of Petrology* **43**, 943–62.

SEN, C. & DUNN, T. 1994. Dehydration melting of a basaltic composition amphibolite at 1.5 and 2.0 GPa – Implications for the origin of adakites. *Contributions to Mineralogy and Petrology* **117**, 394–409.

SPEAR, F. S. 1993. *Metamorphic phase equilibria and pressure–temperature–time paths*. Washington: The Mineralogical Society of America, 799 pp.

STEVENSON, J. A., DACKZO, N. R., CLARKE, G. L., PEARSON, N. & KLEPEIS, K. A. 2005. Direct observation of adakite melts generated in the lower continental crust, Fiordland, New Zealand. *Terra Nova* **17**, 73–9.

TAYLOR, S. R. & MCLENNAN, S. M. 1985. *The continental crust: Its composition and evolution*. Oxford: Blackwell Scientific, 321 pp.

VIELZEUF, D. & SCHMIDT, M. W. 2001. Melting relations in hydrous systems revisited: application to metapelites, metagreywackes and metabasalts. *Contributions to Mineralogy and Petrology* **141**, 251–67.

WOLF, M. B. & WYLLIE, P. J. 1991. Dehydration-melting of solid amphibolite at 10 kbar – textural development, liquid interconnectivity and applications to the segregation of magmas. *Mineralogy and Petrology* **44**, 151–79.

WOLF, M. B. & WYLLIE, P. J. 1993. Garnet growth during amphibolite anatexis – Implications of a garnetiferous restite. *Journal of Geology* **101**, 357–73.

YAMAMOTO, H. & YOSHINO, T. 1998. Superposition of replacements in the mafic granulites of the Jijal complex of the Kohistan arc, northern Pakistan: dehydration and rehydration within deep arc crust. *Lithos* **43**, 219–34.